

---

# README: REpresentation learning by fairness-Aware Disentangling MEmethod

---

**Sungho Park\***

Department of Computer Science  
Yonsei University  
qkrtjdgh18@yonsei.ac.kr

**Dohyung Kim**

Department of Computer Science  
Yonsei University  
dohkim02@yonsei.ac.kr

**Sunhee Hwang**

Department of Computer Science  
Yonsei University  
sunny16@yonsei.ac.kr

**Hyeran Byun**

Department of Computer Science  
Yonsei University  
hrbyun@yonsei.ac.kr

## Abstract

Fair representation learning aims to encode invariant representation with respect to the protected attribute, such as gender or age. In this paper, we design Fairness-aware Disentangling Variational AutoEncoder (FD-VAE) for fair representation learning. This network disentangles latent space into three subspaces with a decorrelation loss that encourages each subspace to contain independent information: 1) target attribute information, 2) protected attribute information, 3) mutual attribute information. After the representation learning, this disentangled representation is leveraged for fairer downstream classification by excluding the subspace with the protected attribute information. We demonstrate the effectiveness of our model through extensive experiments on CelebA and UTK Face datasets. Our method outperforms the previous state-of-the-art method by large margins in terms of equal opportunity and equalized odds.

## 1 Introduction

Artificial Intelligence (AI) is one of the most popular research fields involving computer vision, natural language processing, robotics and etc. Although lots of AI models show a great performance nowadays, several studies find out that the models still output discriminatory outcomes for gender or race [28, 1, 29]. Previous studies define an attribute, which people should not be discriminated against by, as the protected attribute and propose various fairness methods [4, 5, 25, 34, 22, 10]. Some studies of them propose fair representation learning methods that encode fair latent variables in terms of the protected attribute and exploit it for various downstream tasks [31, 34, 32, 22, 10, 2]. Specifically, [7] shows disentangled representation learning [13, 16, 6], which separates the latent variables into several subspaces independent of each other, can be utilized for fair representation learning. They disentangle representation into the subspaces: 1) sensitive latents that have high mutual information with the protected attribute labels and 2) non-sensitive latents that are independent of sensitive latents. Then, only non-sensitive latents are leveraged for downstream classification tasks to achieve fair classification results.

However, as pointed out in [21, 37], it is challenging to learn non-sensitive latents to have discriminative information for downstream target tasks, since it is learned without the supervision of target labels. In addition, we empirically figure out that sensitive latents contain some target attribute information

---

\*qkrtjdgh18@yonsei.ac.kr

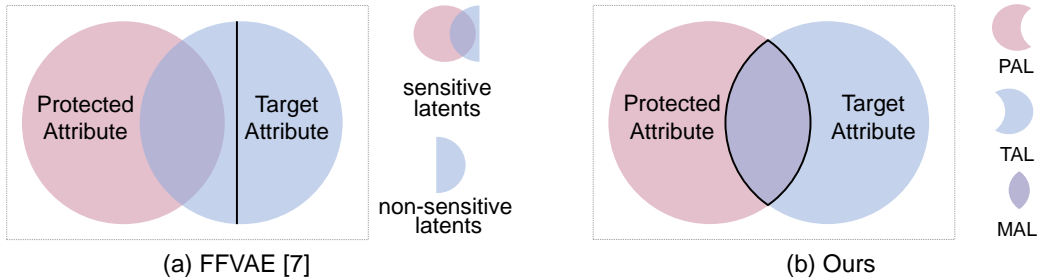


Figure 1: The motivation of our work. The Red circle and blue circle denote information on the protected attribute and target attribute, respectively. This figure conceptually shows how each latent subspace of previous method [7] (sensitive latents and non-sensitive latents) (a) and our method (PAL, TAL, and MAL) include the information. Sensitive latents contain some target attribute information desired to be included in non-sensitive latents

Table 1: Comparison between [7] and ours. We perform downstream classification task on CelebA dataset using each subspace of the previous method [7] (left) and ours (right) for the target and protected attributes. The target attribute (TA) and protected attribute (PA) are set to attractive and male, respectively. Sensitive latents show better classification accuracy on both TA and PA than non-sensitive latents. In ours, on the other hand, TAL and PAL shows better performance than each other on TA and PA, respectively.

|           | FFVAE [7]         |                       | Ours |      |      |
|-----------|-------------------|-----------------------|------|------|------|
|           | sensitive latents | non-sensitive latents | TAL  | PAL  | MAL  |
| TA (Acc.) | 67.4              | 62.7                  | 60.3 | 56.6 | 67.2 |
| PA (Acc.) | 76.7              | 69.1                  | 63.0 | 67.3 | 68.9 |

desired to be included in non-sensitive latents, which is conceptually represented in Figure 1. The experiment is designed to perform downstream classifications using each sensitive and non-sensitive latents. Table 1 shows that classifications using sensitive latents show better performances for both the target and protected attributes than using non-sensitive latents. It indicates that some target attribute information is included in sensitive latents and it is removed since sensitive latents are excluded in downstream tasks.

To mitigate the problem aforementioned, we design a Fairness-aware Disentangling Variational AutoEncoder (FD-VAE). Our method disentangles the latent variables into three independent subspaces: the first subspace is related to the target attribute information (TAL), the second one is related to the protected attribute information (PAL), and the last one is related to the mutual attribute information (MAL). In addition, we propose a decorrelation loss to encourage TAL to have only the target attribute information and PAL to have only the protected attribute information as shown in Figure 1b. MAL encourages to decorrelate the information between TAL and PAL by including the mutual attribute information that is predictive to both the attributes.

When performing downstream classification tasks, we exclude PAL for fair classification with respect to the protected attribute. In addition, we transform MAL into latent variables where the protected attribute information is removed. Then, We utilize TAL and transformed MAL together for a classification, which enables more discriminative classification than using only TAL.

In the experiments section, we compare our method to previous disentangled representation learning methods on CelebA and UTK Face datasets [20, 35]. To evaluate fairness in downstream classification tasks, we utilize two metrics, equal opportunity and equalized odds [12]. In addition, we propose a *equalized accuracy* to measure unbiased classification accuracy on a skewed test dataset. On both the datasets, our method shows the best performance in terms of fairness and comparable performances to previous methods in terms of accuracy. It indicates ours shows better trade-off performances between fairness and accuracy than previous models. In addition, we validate the contribution of each

component of our method through ablation study on CelebA dataset. In short, the main contributions of our paper are as follows:

- We propose a novel FD-VAE to disentangle the latent variables into three independent subspaces related to the target attribute information (TAL), protected attribute information (PAL), and mutual attribute information (MAL).
- We propose a loss that decorrelates information of the target attribute and protected attribute in disentangled latent space.
- We conduct extensive experiments for downstream classification tasks on CelebA and UTK Face datasets. We exploit equal opportunity and equalized odds to evaluate fairness and suggest *equalized accuracy* to evaluate unbiased classification accuracy. Our method outperforms the previous state-of-the-art method by large margins in terms of fairness on both datasets.

## 2 Related Work

### 2.1 Disentangled Representation Learning

Many studies [13, 16, 6, 27, 24, 36, 23, 3, 18] propose disentangled representation learning methods to learn latent variables independent of each other. [13] proves KL-divergence term in the VAE objective function encourages latent variables to be disentangled and proposes  $\beta$ -VAE to weight this term with larger hyperparameter  $\beta (> 1)$ . However, [16] indicates that  $\beta$ -VAE has a trade-off between a disentangling performance and reconstruction quality. To reduce the trade-off, they exploit Total Correlation [30], a measure to estimate the dependency between latent variables, to learn disentangled representation. They approximate it with adversarial learning using discriminator. [6] also optimizes the equivalent objective function to FactorVAE [16] and propose a new stochastic estimation method on Total Correlation, enabling more stable training than FactorVAE.

The concept of disentangled representation is also utilized in various tasks [27, 24, 36, 23, 3, 18]. Disentangling methods for a face recognition [27, 24, 36] separate identity representation from other variations like pose or illumination. They exploit the identity representation for a pose-invariant face recognition. In addition, [23] proposes generation method for person image and disentangles the input image into three factors (foreground, background, and pose) to manipulate those for image generation. [33, 19, 9, 14] learn style translation models to disentangle representation into style and content representations. In this paper, we leverage disentangled representation for fair representation learning

### 2.2 Fair Representation Learning

Fair representation learning aims to learn fair representation in terms of the protected attribute. [31, 34, 32] utilize adversarial learning to remove information related to the protected attribute from representation. [31] formulates a representation learning process as an adversarial minimax game, which optimizes the predictor to output target labels and the discriminator to reduce bias to the protected attribute. [34] propose an adversarial debiasing method to maximize the ability of the predictor for the target class and to minimize the ability of the adversary network for the protected attribute. In addition, [32] proposes FairGAN that generates synthetic data unbiased to the protected attribute and trains classifiers using the generated data. The classifiers show fair classification results on the test dataset composed of real data.

Furthermore, several studies propose fair representation learning methods based on the VAE [22, 2, 7]. Variational fair autoencoder [22] is trained by the penalty term based on Maximum Mean Discrepancy (MMD) [10] and VAE objective function. This method learns representation that is informative on the target label and invariant to the protected attribute. [2] proposes debiasing-VAE (DB-VAE) for a fair face detection. They train the model to identify under-represented data using the latent distribution and adjust the sampling probability of each data to favor the under-represented data. FFVAE [7] is the most similar method to ours. It disentangles representation into sensitive latents and non-sensitive latents. Sensitive latents are learned to include the protected attribute information by the predictiveness term and removed in various downstream classification tasks. In this paper, we find out the limitation that sensitive latents contain some target attribute information with the

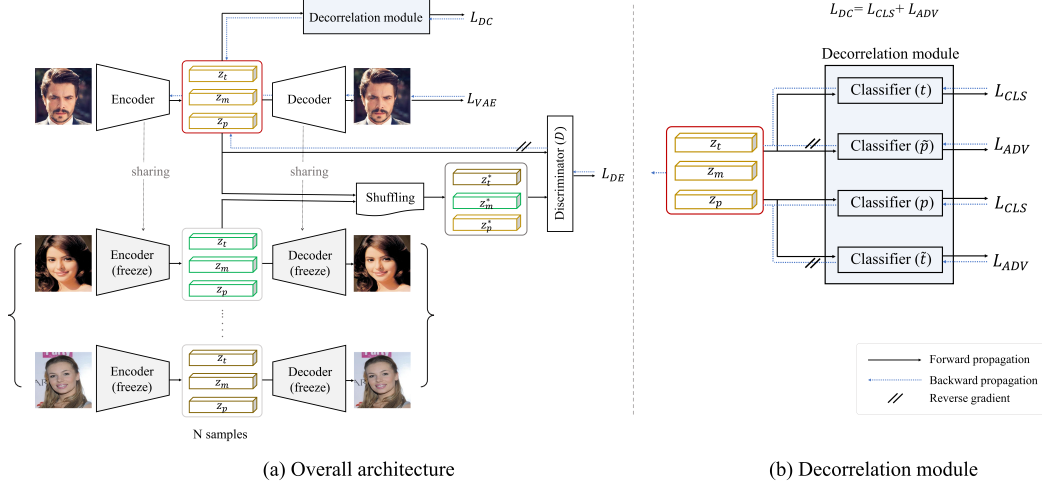


Figure 2: FD-VAE for representation Learning. (a) shows the overall architecture of FD-VAE and (b) shows decorrelation module specifically. PA and TA denote the protected attribute and target attribute, respectively.

protected attribute information since the protected attribute is correlated with other attributes in the real world dataset [26, 11, 25]. Compared to FFVAE, our method explicitly decorrelates information of the protected and target attributes, and mitigates this problem.

### 3 Proposed Method

When observed data  $X = (x_1, \dots, x_n)$ , target attribute labels  $Y_t = (y_{t1}, \dots, y_{tn})$ , and protected attribute labels  $y_p = (y_{p1}, \dots, y_{pn})$  are given, our goal is to learn latent variables  $z$  satisfying three conditions below:

- Maximization of mutual information between  $z$  and  $X$ .
- Disentanglement of  $z$  into three subspaces:  $z_t$  (TAL),  $z_p$  (PAL), and  $z_m$  (MAL).
- Decorrelation between the protected and target attribute information in  $z$ .

To achieve the goals, we design FD-VAE that consist of a VAE network, discriminator, and decorrelation module as shown in Figure 2. We learn our model by maximizing the objective function as follows:

$$L_{TOTAL} = L_{VAE} - \alpha L_{DE} - L_D - L_{DC}, \quad (1)$$

where  $\alpha$  is a hyperparameter and  $L_{VAE}$ ,  $L_{DE}$ ,  $L_D$ , and  $L_{DC}$  denote VAE objective, disentanglement loss, discriminator loss, and decorrelation loss functions, respectively. We specify each loss function in following subsections.

#### 3.1 VAE

Our model is based on variational autoencoder (VAE) [17], which is composed of an encoder and decoder. We learn the VAE network by maximizing the Evidence Lower Bound (ELBO) :

$$L_{VAE} = \sum_{i=1}^n \mathbb{E}_{q_{\Phi}(z_t, z_p, z_m | x_i)} [\log p_{\Theta}(x_i | z_t, z_p, z_m)] - KL[q_{\Phi}(z_t, z_p, z_m | x_i) || p(z_t, z_p, z_m)], \quad (2)$$

where  $\Phi$  and  $\Theta$  are parameters of the encoder and decoder, respectively. The first term of Equation 2 denotes a reconstruction loss that encourages the encoder to map the observed data  $X$  into latent variables  $z$  and the decoder to reconstruct  $X$  from  $z$ . The latent variables  $z$  are sampled from  $q_{\Phi}(z|x) = N(\mu_{q_{\Phi}}(x), \sigma_{q_{\Phi}}(x))$  using the reparameterization trick, where  $\mu$  and  $\sigma$  are the outputs of the encoder. The second term indicates a regularization loss that makes the distribution  $q_{\Phi}(z|x)$  similar to the gaussian prior distribution  $p(z)$  by KL divergence.

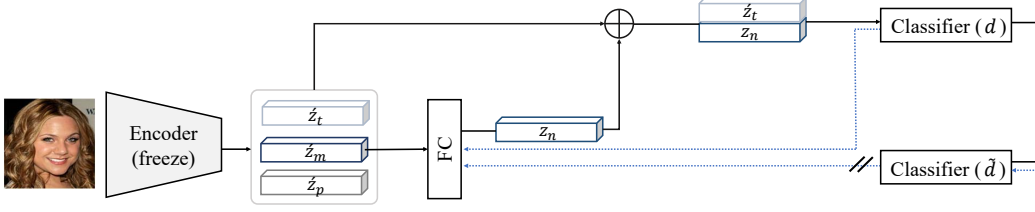


Figure 3: A model for downstream classification tasks. FC denotes a single fully connected layer and  $\oplus$  is element-wise summation.

### 3.2 Disentanglement Loss

To disentangle the latent variables  $z$  into subspaces as  $z_t$ ,  $z_p$ , and  $z_m$ , we minimize Total Correlation [30] by following objective function:

$$L_{DE} = KL[q_{\Phi}(z_t, z_p, z_m) \parallel \prod_{j \subseteq S} q_{\Phi}(z_j)] = \mathbb{E}_{q_{\Phi}(z_t, z_p, z_m)} \left[ \log \frac{q_{\Phi}(z_t, z_p, z_m)}{\prod_{j \subseteq S} q_{\Phi}(z_j)} \right], \quad (3)$$

where  $S = \{t, p, m\}$ . Total Correlation is one of the popular measures that estimate the dependency between latent variables, and it is demonstrated that minimizing this term encourages latent variables to be disentangled [16, 6, 7]. Following the methods in [16, 7], we approximate log density ratio instead of optimizing KL divergence directly by leveraging a discriminator as the following equation:

$$L_{DE} \approx \mathbb{E}_{q_{\Phi}(z_t, z_p, z_m)} \left[ \log \frac{D(z_t, z_p, z_m)}{1 - D(z_t, z_p, z_m)} \right], \quad (4)$$

where  $D(z_t, z_p, z_m)$  is the output probability of the discriminator  $D$  that classifies the samples from  $q_{\Phi}(z_t, z_p, z_m)$  as real and the samples from  $\prod_{j \subseteq S} q_{\Phi}(z_j)$  as fake. The encoder is trained for the discriminator not to classify whether if the samples are real or fake. The fake samples  $z^* = [z_t^*; z_p^*; z_m^*]$  are generated by subspace-wise random shuffling within a mini-batch. The following loss is for training the discriminator:

$$L_D = -\mathbb{E}_{q_{\Phi}(z_t, z_p, z_m)} [\log D(z_t, z_p, z_m) + \log(1 - D(z_t^*, z_p^*, z_m^*))]. \quad (5)$$

### 3.3 Decorrelation Loss

On top of the disentanglement loss that encourages the subspaces to be independent of each other, we introduce a decorrelation loss that specifies which attribute information to be included to each subspace. The decorrelation loss is composed of  $L_{CLS}$  and  $L_{ADV}$  as follows:

$$L_{DC} = \beta L_{CLS} + \gamma L_{ADV}, \quad (6)$$

$$L_{CLS} = -\sum_{i=1}^n \mathbb{E}_{q_{\Phi}(z_t, z_p, z_m | x_i)} [\log p_t(y_t | z_t) + \log p_p(y_p | z_p)], \quad (7)$$

$$L_{ADV} = \max_{\tilde{t}, \tilde{p}} \min_{\Phi} \sum_{i=1}^n \mathbb{E}_{q_{\Phi}(z_t, z_p, z_m | x_i)} [\log p_{\tilde{t}}(y_t | z_t) + \log p_{\tilde{p}}(y_p | z_p)], \quad (8)$$

where  $t$  and  $\tilde{t}$  denote classifiers for the target attribute, and  $p$  and  $\tilde{p}$  denote classifiers for the protected attribute.  $\beta$  and  $\gamma$  are hyperparameters.  $L_{CLS}$  encourages  $z_t$  and  $z_p$  to contain the information of the target attribute and protected attribute, respectively. Meanwhile,  $L_{ADV}$  encourages  $z_t$  and  $z_p$  to exclude information of the protected attribute and target attribute, respectively. However, there is some information that is predictive to both the protected and target attributes. Since the mutual attribute information increases  $L_{ADV}$  whether it is included in  $z_t$  or  $z_p$ , we introduce  $Z_m$  to include this information. There is no additional mapping function on this subspace  $Z_m$ , but  $L_{DE}$  works indirectly.

### 3.4 Downstream Classification Network

After learning a fair representation, we perform downstream classification tasks to predict the target attribute. The overall architecture of our classification model is shown in Figure 3. The loss function to optimize the classification model is defined by:

$$L_{DCLS} = \max_{d,f} \min_{\tilde{d}} \sum_{i=1}^n \mathbb{E}_{q_{\Phi}(z_t, z_p, z'_m | x_i)} [\log p_d(y_t | z_t \oplus f(z'_m)) - \log p_{\tilde{d}}(y_p | f(z'_m))], \quad (9)$$

where  $d$ ,  $\tilde{d}$ , and  $\oplus$  indicate a target attribute classifier, protected attribute classifier, and element-wise summation. The values of the learned latent variables  $z_t$ ,  $z_p$ , and  $z'_m$  are fixed in downstream classification tasks. Firstly, we exclude  $z'_p$  that the protected attribute information is not exploited for downstream classifications. Then,  $z'_m$  is transformed to latent variables  $z_n$  that is irrelevant to the protected attribute by a single fully connected layer  $f$ .  $f$  and  $\tilde{d}$  are learned adversarially for this transformation. Finally,  $z_n$  and  $z_t$  are element-wise summed and feed into  $d$  for a target classification.

## 4 Experiments

### 4.1 Dataset

We validate our contributions on CelebA and UTK datasets. CelebA dataset is consists of about 200k face images with 40 binary attribute annotations and divided into train, validation, and test sets. We set the protected attributes to male and young, and the target attributes to attractive, wavy hair, and big nose. Specifically, we compose four pairs of attributes considering the correlation between the protected and target attributes: [male, attractive], [male, wavy hair], [young, attractive], and [young, big nose].

UTK Face dataset is a face dataset with long age span involving annotations of age, ethnicity, and gender. We set the protected attribute to gender and reclassify the ethnicity annotations into Caucasians and the others, and the age annotations into young and the others(>35). In addition, we divide the dataset into train (10k), validation (2.4k), and test sets (2.4k). In detail, we compose the train set to have a correlation between the protected and target attributes for fairness study. In respect to the ethnicity, one-fifth of Caucasians are female and four-fifths are male, and the others have the opposite ratio. Likewise, in respect to the age, one-fifth of young are male and four-fifths are female, and the others have the opposite ratio. In addition, we set both the datasets for validation and test to be balanced sets (cf. Appendix A).

### 4.2 Evaluation Metrics

As metrics for fairness, we use equal opportunity and equalized odds which are defined as  $|\text{TPR}_{p_0} - \text{TPR}_{p_1}|$  and  $\frac{1}{2}[|\text{TPR}_{p_0} - \text{TPR}_{p_1}| + |\text{TNR}_{p_0} - \text{TNR}_{p_1}|]$ , respectively, where  $p_1$  are data with the positive protected attribute and  $p_0$  are vice versa. TPR and TNR are the abbreviation of true positive rate and true negative rate, respectively.

In addition, we suggest *equalized accuracy* to evaluate unbiased classification accuracy. If train and test set have similar data distributions, the standard accuracy metric benefits models biased to the distribution of train set. On UTK Face dataset, we solve this problem by comprising a balanced test set, but CelebA dataset provides a fixed test set. Alternatively, we introduce *equalized accuracy* which has the same effect as the balanced set. This metric is defined as:  $\frac{1}{4}[\text{TPR}_{p_0} + \text{TNR}_{p_0} + \text{TPR}_{p_1} + \text{TNR}_{p_1}]$ . More details on *equalized accuracy* are described in Appendix B.

### 4.3 Implementation Details

The detailed structures of our networks are specified in Appendix C. In our model, TAL, PAL, and MAL are set to 20 dimensions, respectively. In addition, for fair comparison, the representation of all models are set to 60 dimensions. The dimension of sensitive latents and non-sensitive latents in FFVAE are divided into 30. For downstream classification tasks, we remove one or two latents the most correlated with the protected attribute in FactorVAE and *beta*-VAE as in [7]. The hyperparameters  $\alpha$ ,  $\beta$ , and  $\gamma$  are fixed to 50, 5 and 10, respectively.

Table 2: Classification results on CelebA dataset. TA and PA are the abbreviations of the target attribute and protected attribute. We utilize four metrics: equal opportunity (Opp.), equalized odds (Odds), accuracy (ACC.), and *equalized accuracy* (EAcc.). M,Y,A,W and B denote male, young, attractive, wavy hair, and big nose attributes, respectively.

| Method            | TA  | PA   |      | Opp. ↓      | Odds ↓     | Acc. ↑<br>EAcc. ↑ | TA  | PA   |      | Opp. ↓     | Odds ↓     | Acc. ↑<br>EAcc. ↑ |
|-------------------|-----|------|------|-------------|------------|-------------------|-----|------|------|------------|------------|-------------------|
|                   |     | M=1  | M=0  |             |            |                   |     | Y=1  | Y=0  |            |            |                   |
| VAE [17]          | A=1 | 54.3 | 81.5 | 27.2        | 28.7       | 70.6              | A=1 | 77.4 | 67.6 | 9.7        | 11.3       | 70.9              |
|                   | A=0 | 77.8 | 47.5 |             |            |                   | A=0 | 60.8 | 72.7 |            |            |                   |
| $\beta$ -VAE [13] | A=1 | 57.7 | 78.8 | 21.1        | 22.1       | 68.7              | A=1 | 72.9 | 65.6 | 7.2        | 5.8        | 67.5              |
|                   | A=0 | 73.1 | 48.8 |             |            |                   | A=0 | 61.1 | 65.4 |            |            |                   |
| FactorVAE [16]    | A=1 | 59.7 | 80.4 | 20.7        | 23.4       | 69.0              | A=1 | 76.0 | 66.8 | 9.2        | 9.1        | 68.9              |
|                   | A=0 | 72.8 | 46.6 |             |            |                   | A=0 | 58.9 | 68.1 |            |            |                   |
| FFVAE [7]         | A=1 | 54.9 | 73.4 | 17.7        | 17.5       | 62.7              | A=1 | 70.4 | 62.3 | 8.0        | 8.2        | 64.2              |
|                   | A=0 | 63.3 | 46.5 |             |            |                   | A=0 | 55.3 | 63.6 |            |            |                   |
| Ours              | A=1 | 66.2 | 67.6 | <b>1.3</b>  | <b>4.9</b> | 64.1              | A=1 | 76.5 | 72.7 | <b>3.7</b> | <b>1.9</b> | 65.5              |
|                   | A=0 | 64.4 | 55.8 |             |            |                   | A=0 | 59.4 | 55.2 |            |            |                   |
| VAE [17]          | W=1 | 5.5  | 52.7 | 47.1        | 33.4       | 73.0              | B=1 | 58.5 | 75.5 | 17.0       | 19.2       | 67.2              |
|                   | W=0 | 98.7 | 79.0 |             |            |                   | B=0 | 71.6 | 50.2 |            |            |                   |
| $\beta$ -VAE [13] | W=1 | 6.6  | 42.1 | 35.4        | 15.3       | 70.7              | B=1 | 55.0 | 67.4 | 12.3       | 13.9       | 65.0              |
|                   | W=0 | 98.0 | 82.6 |             |            |                   | B=0 | 69.2 | 53.6 |            |            |                   |
| FactorVAE [16]    | W=1 | 8.1  | 47.5 | 38.8        | 28.8       | 71.0              | B=1 | 56.0 | 69.2 | 13.2       | 14.4       | 64.8              |
|                   | W=0 | 97.6 | 78.7 |             |            |                   | B=0 | 68.6 | 53.0 |            |            |                   |
| FFVAE [7]         | W=1 | 4.5  | 25.7 | 21.1        | 15.4       | 67.7              | B=1 | 50.8 | 56.2 | 5.3        | 8.5        | 63.0              |
|                   | W=0 | 98.4 | 88.7 |             |            |                   | B=0 | 67.3 | 58.7 |            |            |                   |
| Ours              | W=1 | 3.8  | 17.2 | <b>13.4</b> | <b>8.9</b> | 66.1              | B=1 | 48.2 | 47.5 | <b>1.2</b> | <b>1.5</b> | 63.9              |
|                   | W=0 | 97.5 | 93.1 |             |            |                   | B=0 | 69.6 | 62.6 |            |            |                   |

Table 3: Classification results on UTK Face dataset. G,E, and A indicate gender (1:male, 0:female), ethnicity (1:Caucasian, 0:others), and age (1:young, 0:old), respectively.

| Method            | TA  | PA   |      | Opp. ↓     | Odds ↓     | Acc. ↑ | TA  | PA   |      | Opp. ↓     | Odds ↓     | Acc. ↑ |
|-------------------|-----|------|------|------------|------------|--------|-----|------|------|------------|------------|--------|
|                   |     | G=1  | G=0  |            |            |        |     | E=1  | E=0  |            |            |        |
| VAE [17]          | E=1 | 70.5 | 54.3 | 16.1       | 17.4       | 65.2   | A=1 | 50.8 | 75.5 | 24.6       | 29.8       | 60.7   |
|                   | E=0 | 58.6 | 77.4 |            |            |        | A=0 | 75.8 | 40.7 |            |            |        |
| $\beta$ -VAE [13] | E=1 | 72.1 | 59.4 | 12.7       | 12.1       | 60.1   | A=1 | 45.3 | 62.5 | 17.1       | 20.8       | 54.3   |
|                   | E=0 | 48.7 | 60.2 |            |            |        | A=0 | 67.1 | 42.5 |            |            |        |
| FactorVAE [16]    | E=1 | 72.5 | 60.3 | 12.1       | 12.9       | 59.4   | A=1 | 43.5 | 66.7 | 23.2       | 27.1       | 54.6   |
|                   | E=0 | 45.8 | 59.5 |            |            |        | A=0 | 69.6 | 38.5 |            |            |        |
| FFVAE [7]         | E=1 | 65.1 | 55.2 | 9.8        | 9.1        | 59.7   | A=1 | 45.2 | 58.9 | 13.6       | 17.2       | 54.5   |
|                   | E=0 | 54.8 | 64.0 |            |            |        | A=0 | 67.4 | 46.5 |            |            |        |
| Ours              | E=1 | 65.8 | 63.5 | <b>2.3</b> | <b>1.1</b> | 60.3   | A=1 | 47.9 | 45.8 | <b>2.0</b> | <b>2.9</b> | 54.1   |
|                   | E=0 | 56.0 | 56.0 |            |            |        | A=0 | 63.3 | 59.4 |            |            |        |

#### 4.4 Evaluation

To validate our method, we compare ours with previous methods [13, 16, 7]. Table 2 shows the classification results on CelebA dataset. VAE (baseline), which does not consider the disentanglement of latent variables, shows the unfairest performance in all the experiments. The two disentangling methods  $\beta$ -VAE [13] and FactorVAE [16] improve fairness of results than the baseline. However, it is not significant since they do not leverage the protected attribute in the disentanglement process. FFVAE [7], which is the state-of-the-art method, achieves better results in terms of both equal opportunity and equalized odds than the other previous methods. Our method shows the fairest performance in all the experiments and outperforms FFVAE by large margins of 16.4%, 7.7%, 4.3%, and 3.1% at equal opportunity and 12.6%, 6.5%, 6.3%, and 7.0% at equalized odds. In terms of accuracy and *equalized accuracy*, ours shows similar performances to FFVAE, and it indicates ours has better trade-off performances between fairness scores and classification accuracy.

The results on UTK Face dataset are shown in Table 3. Similar to the above, VAE (baseline) shows highly unfair results in terms of both equal opportunity and equalized odds, and the previous methods [13, 16, 7] improve fairness scores over the baseline. Our method significantly surpasses the previous methods, showing 2.3% and 1.1% at equal opportunity, and 2.0% and 2.9% at equalized odds.

Table 4: Ablation Study on CelebA dataset. We set FFVAE [7] to the baseline (first row).  $z_m$  denotes MAL in representation learning and  $z_t, z'_m$ , and  $z_n$  denote learned TAL, MAL, and transformed MAL in the downstream classification, respectively. We set the protected attribute to Male (M) and the target attribute to Attractive (A) in this experiment.

| Representation learning |           |       | Downstream Classification |        |       | TA       | PA   |            | Opp. ↓     | Odds ↓ | Acc. ↑ |
|-------------------------|-----------|-------|---------------------------|--------|-------|----------|------|------------|------------|--------|--------|
| $L_{CLS}$               | $L_{ADV}$ | $z_m$ | $z_t$                     | $z'_m$ | $z_n$ |          | M=1  | M=0        |            |        |        |
|                         |           |       | ✓                         |        |       | A=1 54.9 | 73.4 | 17.7       | 17.5       | 62.7   |        |
|                         |           |       |                           |        |       | A=0 63.3 | 46.5 |            |            |        |        |
| ✓                       |           |       | ✓                         |        |       | A=1 60.7 | 76.4 | 15.6       | 16.2       | 65.3   |        |
|                         |           |       |                           |        |       | A=0 64.2 | 47.3 |            |            |        |        |
| ✓                       | ✓         |       | ✓                         |        |       | A=1 75.7 | 72.3 | 3.4        | 5.7        | 64.1   |        |
|                         |           |       |                           |        |       | A=0 58.7 | 50.8 |            |            |        |        |
| ✓                       | ✓         | ✓     | ✓                         |        |       | A=1 68.1 | 66.3 | 1.8        | <b>2.1</b> | 60.3   |        |
|                         |           |       |                           |        |       | A=0 55.1 | 52.6 |            |            |        |        |
| ✓                       | ✓         | ✓     | ✓                         | ✓      |       | A=1 57.9 | 77.7 | 19.8       | 20.8       | 67.1   |        |
|                         |           |       |                           |        |       | A=0 69.8 | 47.8 |            |            |        |        |
| ✓                       | ✓         | ✓     | ✓                         |        | ✓     | A=1 66.2 | 67.6 | <b>1.3</b> | 4.9        | 64.1   |        |
|                         |           |       |                           |        |       | A=0 64.4 | 55.8 |            |            |        |        |

In conclusion, the experiments on the two datasets indicate that our method decorrelates information of the protected attribute and target attribute better than the others, which causes superior trade-off performance between fairness scores and classification accuracy.

#### 4.5 Ablation Study

We conduct ablation study on CelebA dataset to validate the contribution of each component of our method. We set FFVAE [7] to a baseline in this experiment and added each component step by step. The results are shown in Table 4. Firstly, we add  $L_{CLS}$  term of the decorrelation loss, which trains TAL by the supervision with the target attribute labels. As a result, classification accuracy and fairness scores are improved than the baseline model. Secondly, we add the total decorrelation loss ( $L_{CLS}+L_{ADV}$ ). The information between the target and protected attributes is more clearly decorrelated than using  $L_{CLS}$  term only. It significantly improves fairness scores by 12.2% and 10.5% in equal opportunity and equalized odds, respectively.

Then, we experiment three models added with MAL ( $z_m$ ) in representation learning. The first model utilizes only TAL ( $z_t$ ) in the downstream classification task. In addition, the second and final models use MAL ( $z'_m$ ) or transformed MAL ( $z_n$ ) with TAL, respectively. The first model demonstrates that MAL helps to exclude the protected attribute information from TAL, showing the lowest fairness scores. However, it degrades classification accuracy since the mutual attribute information is not utilized for classification. The second and final models show that the transformation of  $z'_m$  is effective. Although utilizing learned MAL without the transformation improves classification accuracy, it highly degrades fairness scores. The final model (FD-VAE) improves classification accuracy while maintaining outstanding fairness scores.

## 5 Conclusion

In this paper, we introduced the Fairness-aware Disentangling Variational Auto Encoder (FD-VAE) that disentangles latent variables into three subspaces including information of the target attribute, protected attribute, and mutual attribute, respectively. By excluding the subspace with protected attribute information, we performed fair downstream classification tasks. In all the experiments on CelebA and UTK datasets, our method achieved the fairest results in terms of equal opportunity and equalized odds.

### Broader Impact

This work mitigates ethical-social problems caused by Artificial Intelligence (AI) models. Previous AI models have caused social discrimination, such as racism or sexism. For example, Google Photos, one of the visual recognition applications, recognized a couple of African-Americans as a gorilla [8].



Moreover, Compas algorithm, which is used to predict recidivism by courts in the United States, has judged unfairly on African-American [15]. Our method separates information causing such the discrimination from data representation and makes a fair decision. In addition, our fair representation can be applied to various tasks that the fairness of the results is required. Therefore, our study has a positive impact that mitigates the problems of prejudice in AI models and enables individuals to have fair and plentiful benefits.

## Acknowledgments and Disclosure of Funding

TBD.

## References

- [1] M. S. Alvi, A. Zisserman, and C. Nellåker. Turning a blind eye: Explicit removal of biases and variation from deep neural network embeddings. In L. Leal-Taixé and S. Roth, editors, *Computer Vision - ECCV 2018 Workshops - Munich, Germany, September 8-14, 2018, Proceedings, Part I*, volume 11129 of *Lecture Notes in Computer Science*, pages 556–572. Springer, 2018. doi: 10.1007/978-3-030-11009-3\_34. URL [https://doi.org/10.1007/978-3-030-11009-3\\_34](https://doi.org/10.1007/978-3-030-11009-3_34).
- [2] A. Amini, A. P. Soleimany, W. Schwarting, S. N. Bhatia, and D. Rus. Uncovering and mitigating algorithmic bias through learned latent structure. In *Proceedings of the 2019 AAAI/ACM Conference on AI, Ethics, and Society*, AIES '19, page 289–295, New York, NY, USA, 2019. Association for Computing Machinery. ISBN 9781450363242. doi: 10.1145/3306618.3314243. URL <https://doi.org/10.1145/3306618.3314243>.
- [3] S. Bi, K. Sunkavalli, F. Perazzi, E. Shechtman, V. G. Kim, and R. Ramamoorthi. Deep cg2real: Synthetic-to-real translation via image disentanglement. In *The IEEE International Conference on Computer Vision (ICCV)*, October 2019.
- [4] T. Bolukbasi, K.-W. Chang, J. Zou, V. Saligrama, and A. Kalai. Man is to computer programmer as woman is to homemaker? debiasing word embeddings. In *Proceedings of the 30th International Conference on Neural Information Processing Systems*, NIPS'16, page 4356–4364, Red Hook, NY, USA, 2016. Curran Associates Inc. ISBN 9781510838819.
- [5] K. Burns, L. A. Hendricks, T. Darrell, and A. Rohrbach. Women also snowboard: Overcoming bias in captioning models. In *ECCV*, 2018.
- [6] R. T. Q. Chen, X. Li, R. B. Grosse, and D. K. Duvenaud. Isolating sources of disentanglement in variational autoencoders. In S. Bengio, H. Wallach, H. Larochelle, K. Grauman, N. Cesa-Bianchi, and R. Garnett, editors, *Advances in Neural Information Processing Systems 31*, pages 2610–2620. Curran Associates, Inc., 2018. URL <http://papers.nips.cc/paper/7527-isolating-sources-of-disentanglement-in-variational-autoencoders.pdf>.
- [7] E. Creager, D. Madras, J.-H. Jacobsen, M. Weis, K. Swersky, T. Pitassi, and R. Zemel. Flexibly fair representation learning by disentanglement. In K. Chaudhuri and R. Salakhutdinov, editors, *Proceedings of the 36th International Conference on Machine Learning*, volume 97 of *Proceedings of Machine Learning Research*, pages 1436–1445, Long Beach, California, USA, 09–15 Jun 2019. PMLR. URL <http://proceedings.mlr.press/v97/creager19a.html>.
- [8] C. Dougherty. Google photos mistakenly labels black people gorillas. 2015. URL <https://bits.blogs.nytimes.com/2015/07/01/google-photos-mistakenly-labels-black-people-gorillas>.
- [9] A. Gonzalez-Garcia, J. v. d. Weijer, and Y. Bengio. Image-to-image translation for cross-domain disentanglement. In *Proceedings of the 32nd International Conference on Neural Information Processing Systems*, NIPS'18, page 1294–1305, Red Hook, NY, USA, 2018. Curran Associates Inc.

- [10] A. Gretton, K. Borgwardt, M. Rasch, B. Schölkopf, and A. J. Smola. A kernel method for the two-sample-problem. In B. Schölkopf, J. C. Platt, and T. Hoffman, editors, *Advances in Neural Information Processing Systems 19*, pages 513–520. MIT Press, 2007. URL <http://papers.nips.cc/paper/3110-a-kernel-method-for-the-two-sample-problem.pdf>.
- [11] E. M. Hand and R. Chellappa. Attributes for improved attributes: A multi-task network utilizing implicit and explicit relationships for facial attribute classification. In *Proceedings of the Thirty-First AAAI Conference on Artificial Intelligence, AAAI’17*, page 4068–4074. AAAI Press, 2017.
- [12] M. Hardt, E. Price, and N. Srebro. Equality of opportunity in supervised learning. In *Proceedings of the 30th International Conference on Neural Information Processing Systems, NIPS’16*, page 3323–3331, Red Hook, NY, USA, 2016. Curran Associates Inc. ISBN 9781510838819.
- [13] I. Higgins, L. Matthey, A. Pal, C. Burgess, X. Glorot, M. M. Botvinick, S. Mohamed, and A. Lerchner. beta-vae: Learning basic visual concepts with a constrained variational framework. In *ICLR*, 2017.
- [14] X. Huang, M.-Y. Liu, S. J. Belongie, and J. Kautz. Multimodal unsupervised image-to-image translation. In *ECCV*, 2018.
- [15] S. M. J. Angwin, J. Larson and L. Kirchner. Machine bias: There’s software used across the country to predict future criminals. and it’s biased against blacks. ProPublica, 2016. URL <https://www.propublica.org/article/machine-bias-risk-assessments-in-criminal-sentencing>.
- [16] H. Kim and A. Mnih. Disentangling by factorising. In J. Dy and A. Krause, editors, *Proceedings of the 35th International Conference on Machine Learning*, volume 80 of *Proceedings of Machine Learning Research*, pages 2649–2658, Stockholmsmässan, Stockholm Sweden, 10–15 Jul 2018. PMLR.
- [17] D. P. Kingma and M. Welling. Auto-encoding variational bayes. In Y. Bengio and Y. LeCun, editors, *2nd International Conference on Learning Representations, ICLR 2014, Banff, AB, Canada, April 14-16, 2014, Conference Track Proceedings*, 2014. URL <http://arxiv.org/abs/1312.6114>.
- [18] D. Kotovenko, A. Sanakoyeu, S. Lang, and B. Ommer. Content and style disentanglement for artistic style transfer. In *Proceedings of the IEEE International Conference on Computer Vision*, pages 4422–4431, 2019.
- [19] H. Lee, H. Tseng, J. Huang, M. Singh, and M. Yang. Diverse image-to-image translation via disentangled representations. In M. Hebert, V. Ferrari, C. Sminchisescu, and Y. Weiss, editors, *Computer Vision – ECCV 2018 - 15th European Conference, 2018, Proceedings*, Lecture Notes in Computer Science (including subseries Lecture Notes in Artificial Intelligence and Lecture Notes in Bioinformatics), pages 36–52, Germany, Jan. 2018. Springer Verlag. ISBN 9783030012458. doi: 10.1007/978-3-030-01246-5\_3. 15th European Conference on Computer Vision, ECCV 2018 ; Conference date: 08-09-2018 Through 14-09-2018.
- [20] Z. Liu, P. Luo, X. Wang, and X. Tang. Deep learning face attributes in the wild. In *Proceedings of International Conference on Computer Vision (ICCV)*, December 2015.
- [21] C. Louizos, K. Swersky, Y. Li, M. Welling, and R. S. Zemel. The variational fair autoencoder. In Y. Bengio and Y. LeCun, editors, *4th International Conference on Learning Representations, ICLR 2016, San Juan, Puerto Rico, May 2-4, 2016, Conference Track Proceedings*, 2016. URL <http://arxiv.org/abs/1511.00830>.
- [22] C. Louizos, K. Swersky, Y. Li, M. Welling, and R. S. Zemel. The variational fair autoencoder. *CoRR*, abs/1511.00830, 2016.
- [23] L. Ma, Q. Sun, S. Georgoulis, L. Van Gool, B. Schiele, and M. Fritz. Disentangled person image generation. In *Proceedings of the IEEE Conference on Computer Vision and Pattern Recognition*, pages 99–108, 2018.

- [24] X. Peng, X. Yu, K. Sohn, D. N. Metaxas, and M. Chandraker. Reconstruction-based disentanglement for pose-invariant face recognition. In *2017 IEEE International Conference on Computer Vision (ICCV)*, pages 1632–1641, 2017.
- [25] K. V. K. Singh, D. K. Mahajan, K. Grauman, Y. J. Lee, M. Feiszli, and D. Ghadiyaram. Don’t judge an object by its context: Learning to overcome contextual bias. *ArXiv*, abs/2001.03152, 2020.
- [26] R. Torfason, E. Agustsson, R. Rothe, and R. Timofte. From face images and attributes to attributes. In *ACCV*, 2016.
- [27] L. Tran, X. Yin, and X. Liu. Disentangled representation learning gan for pose-invariant face recognition. In *2017 IEEE Conference on Computer Vision and Pattern Recognition (CVPR)*, pages 1283–1292, 2017.
- [28] M. Wang, W. Deng, J. Hu, X. Tao, and Y. Huang. Racial faces in the wild: Reducing racial bias by information maximization adaptation network. In *The IEEE International Conference on Computer Vision (ICCV)*, October 2019.
- [29] T. Wang, J. Zhao, M. Yatskar, K.-W. Chang, and V. Ordonez. Balanced datasets are not enough: Estimating and mitigating gender bias in deep image representations. *2019 IEEE/CVF International Conference on Computer Vision (ICCV)*, pages 5309–5318, 2019.
- [30] S. Watanabe. Information theoretical analysis of multivariate correlation. *IBM J. Res. Dev.*, 4(1):66–82, Jan. 1960. ISSN 0018-8646. doi: 10.1147/rd.41.0066. URL <https://doi.org/10.1147/rd.41.0066>.
- [31] Q. Xie, Z. Dai, Y. Du, E. Hovy, and G. Neubig. Controllable invariance through adversarial feature learning. In *Proceedings of the 31st International Conference on Neural Information Processing Systems, NIPS’17*, page 585–596, Red Hook, NY, USA, 2017. Curran Associates Inc. ISBN 9781510860964.
- [32] D. Xu, S. Yuan, L. Zhang, and X. Wu. Fairgan: Fairness-aware generative adversarial networks. pages 570–575, 12 2018. doi: 10.1109/BigData.2018.8622525.
- [33] X. Yu, Y. Chen, T. H. Li, S. Liu, and G. Li. Multi-mapping image-to-image translation via learning disentanglement. In *NeurIPS*, 2019.
- [34] B. H. Zhang, B. Lemoine, and M. Mitchell. Mitigating unwanted biases with adversarial learning. In *Proceedings of the 2018 AAAI/ACM Conference on AI, Ethics, and Society, AIES ’18*, page 335–340, New York, NY, USA, 2018. Association for Computing Machinery. ISBN 9781450360128. doi: 10.1145/3278721.3278779. URL <https://doi.org/10.1145/3278721.3278779>.
- [35] S. Y. Zhang, Zhifei and H. Qi. Age progression/regression by conditional adversarial autoencoder. In *IEEE Conference on Computer Vision and Pattern Recognition (CVPR)*. IEEE, 2017.
- [36] Z. Zhu, P. Luo, X. Wang, and X. Tang. Multi-view perceptron: a deep model for learning face identity and view representations. In *NIPS*, 2014.
- [37] F. Zhuang, X. Cheng, P. Luo, S. J. Pan, and Q. He. Supervised representation learning: Transfer learning with deep autoencoders. In *Proceedings of the 24th International Conference on Artificial Intelligence, IJCAI’15*, page 4119–4125. AAAI Press, 2015. ISBN 9781577357384.